New composites for neutron radiation shielding

Franco Cataldo[1] · Michele Prata[2]

Abstract

A castable polyurethane (PUR) with soft segment made by polytetrahydrofuran polyol (or polytretramethylene ether glycol = PTMEG) derived from renewable sources was used as polymer matrix to prepare neutron shields. The PUR polymer matrix was filled with 20.4% of amorphous boron or with 20.9% by weight of hexagonal boron nitride (h-BN). The PUR composites were cast in foils 2 mm thick and tested as thermal neutron shields against reference unfilled PUR foils. The method of sandwitched copper wire activation till saturation was used for the determination of the neutron shielding effectiveness. Both the linear and massic attenuation coefficient of the two PUR composites were determined. Making 100 the linear attenuation coefficient μ of unfilled PUR, the μ value of 20.4% amorphous boron filled composite was found at 224 while that of 20.9% filled BN was found at 182. Making 100 the mass attenuation coefficient μ/ρ of the unfilled PUR the amorphous boron PUR filled composite was found at 311 while the BN filled PUR composite stopped at 178. Unfilled PUR and PUR composites were studied with FT-IR spectroscopy and DSC before and after neutron processing with a total dose of 1.5×10^{13} cm^{-2}. No significant changes were detected neither in the FT-IR spectra nor in the DSC thermal behaviour confirming the excellent radiation resistance of PUR and its suitability as polymer matrix for neutrons and more in general radiation shielding.

Keywords Polyurethane composites · Neutrons · Radiation shielding · Boron · FT-IR · DSC

Introduction

Reliable radiation shielding materials are requested both for traditional applications i.e. X-ray shielding in medical and industrial radiology, shielding in nuclear medicine, cyclotrons as well as in fission nuclear reactors, and nuclear waste removal, processing and storage [1–3], but also for emerging and challenging applications such as space radiation shielding especially for long term manned missions [4–7] and neutron streaming from fusion Tokamak reactors [8].

Limiting the introduction to composites for shielding space radiation in the case of manned missions, according to a NASA document [9], the action of cosmic rays and/or solar wind on the metallic shell of a common spacecraft produces cascade neutrons which are directed in the interior part of the spacecraft and contribute significantly to the radiation dose absorbed by the crew in a deep space mission. The traditional spacecraft building material is based on aluminum and in Apollo mission the external spacecraft building consisted of an Al skin followed by an internal layer of steel honeycomb and by another layer of internal Al surface. The irradiation of Al and Fe with cosmic rays and solar wind particles (especially those from SPE = Solar Particles Events) produces a series of secondary protons and neutrons directed toward the inner part of the spacecraft. The secondary protons can undergo capture by nuclei without the necessary emission of a new nuclear fragment but only with the emission of γ quanta [10, 11]. Only when protons have very high energy > 50 MeV, then nuclear reactions occur with the production of secondary neutrons [10, 11]. Relativistic protons for example at 1–3 GeV can give rise to spallation reactions like for instance [10, 11]:

$$^{27}\text{Al} + \text{p} \rightarrow 10\text{p} + 11\text{n} + {}^{7}\text{Be}$$
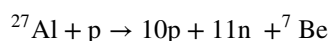
where from the Al disintegration an avalanche of protons and neutrons are produced. The mentioned reaction is applicable to a spacecraft in deep space mission. Similarly, for

✉ Franco Cataldo
franco.cataldo@fastwebnet.it

[1] Actinium Chemical Research Institute, Via Casilina 1626A, 00133 Rome, Italy

[2] Laboratorio Energia Nucleare Applicata, Università degli Studi di Pavia, Via Aselli 41, 27100 Pavia, Italy
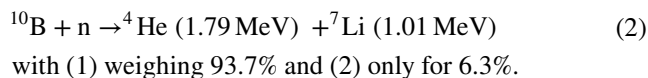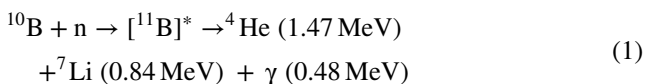
^{56}Fe nuclei even protons of only 340 MeV can cause a spallation reaction on ^{56}Fe [10, 11].

Based on these considerations, the NASA paper [9] strongly suggests that there is the need to study passive radiation shielding toward neutrons to protect the crew in deep space mission.

It should be outlined that simple composites-based shielding materials were proposed since long time [12]. Especially polyethylene (PE) and polymethylmethacrylate (PMMA) where proposed as polymeric matrices for radiation shielding as internal layers inside the spacecraft [12]. More in detail, loading of these polymeric matrices with neutrons adsorbing materials such as graphite and boron carbide were already proposed and tested [12]. However, PE can accept a really limited loading of filler before losing its mechanical properties and the already limited flexibility. Furthermore, PE is not suitable at all as polymeric matrix to be composed with reinforcing and shielding textile fabric. On the other hand, PMMA is already known to be less effective than PE as shielding material and limitation occurs also in this case for the maximum filler loading to keep acceptable mechanical properties [12]. The major drawback for PE and PMMA is also the limitations in radiation resistance. Each polymer exposed to high energy radiation undergoes crosslinking reactions and chain scission. Unfortunately, for both PE but especially for PMMA the chain scission reactions prevail over crosslinks [13]. Currently, the main focus on composites for radiation shielding relies on PE which remains a very popular polymer matrix [14], conjugated under various grades such as HDPE [15–20], LLDPE [21] and UHMWPE [22] as well as UHMWPE fibers in epoxy composite [23]. Other polymer matrices studied much less frequently are EPDM [24–27], nitrile rubber [28], natural rubber [29–31], styrene-butadiene rubber [32] and silicon rubber [33]. Furthermore, apart the well known rigid epoxy-based composites [14], also quite unusual flexible epoxy composites were studied as well [34].

Regarding the fillers used in the composite, graphite and graphite-based fabrics were used [35] mainly to slow down fast neutrons while for neutron capture the most preferrend compounds are boron compounds and in particular boric acid (H_3BO_3) which is the most economic, followed by boron carbide B_4C and boron nitride BN.

Natural elemental boron is composed by a mixture of about 20% ^{10}B isotope and by about 80% of ^{11}B isotope, and it is characterized by a thermal neutron absorption cross-section of 760 barn, which reaches 3890 barn in the case of pure ^{10}B isotope [36]. The thermal neutron capture reaction of ^{10}B can be summarized as follows [36, 37]:

$$^{10}B + n \rightarrow [^{11}B]^* \rightarrow {}^4He\,(1.47\,MeV)$$
$$+ {}^7Li\,(0.84\,MeV)\,+\,\gamma\,(0.48\,MeV) \tag{1}$$

$$^{10}B + n \rightarrow {}^4He\,(1.79\,MeV)\,+{}^7Li\,(1.01\,MeV) \tag{2}$$

with (1) weighing 93.7% and (2) only for 6.3%.

In a series of previous works, Cataldo et al. have studied the effect of neutrons and other high energy radiations on a series of boron compounds suitable to be used as fillers in nanocomposites [36–47]. In particular, hexagonal boron nitride [36], boron carbide (represented as $B_{12}C_3$ or B_4C) [37, 38], the salt lithium bis oxalate-borate (known as LiBOB) [39], graphite [40, 41], fullerenes [42–45], nanodiamonds [46] and single wall carbon nanohorns [47] were studied after neutron or γ rays irradiation.

Castable polyurethanes as polymer matrix for radiation shielding composites were not reported in literature to the best of our knowledge. Consequently, the present work is dedicated to the preparation of polyurethane-based nanocomposites filled with micronized fillers made by hexagonal boron nitride and amorphous boron. The resulting composites were studied as radiation shield in the attenuation of an essentially thermal neutron field produced in the research nuclear reactor installed at the University of Pavia, Italy.

Experimental

Materials and equipment

Polytetrahydrofuran polyol [known also as poly(tetramethylene ether) glycol = PTMEG or poly(tetramethylene oxide)] was obtained from Merck-Aldrich (Germany-USA), characterized by a viscosity of 800 cPs and density of 1.05 g/ml. The 1,1-diphenylmethane diisocyanate polyol pre-polymer was instead a commercial grade characterized by a viscosity of 260 cPs and density of 1.19 g/ml.

All fillers were purchased from Merck-Aldrich (Germany–USA). Boron nitride (BN) was characterized by particle size ≤ 1 μm; the same applies to the sample of amorphous boron with particle size ≤ 1 μm.

The FT-IR spectra on pristine and neutron-processed composites were recorded on a Nicolet 6700 spectrometer from Thermo-Scientific, in reflectance mode using ZnSe crystal as window. The Omnic software of the FT-IR spectrometer was used to convert the reflectance spectra collected into the absorbance spectra.

The DSC analysis was performed on a Mettler-Toledo DSC-1 Star System using conventional Al crucibles with punched caps at a heating rate of 10 °C/min under nitrogen flow.

Preparation of composites

The polyether-polyurethane (PUR) composites were prepared by loading the filler into the polytetrahydrofuran polyol, mixing thoroughly with a large spatula until the

complete filler incorporation and then pouring the second component, i.e. the 1,1-diphenylmethane diisocyanate polyol pre-polymer into the mixture with the filler. Once completed the mixing and homogenization of the three components, the mixture was poured into a 12×12 cm squarred silicon template (in general it works also with an Al template as well as with enamelled steel). The compound was left to cure at room temperature for a couple of days before removal from the template as free standing foil 2 mm thick.

For each compound, the typical composition by weight was as follows: 56% of polytetrahydrofuran polyol, 21% of filler and 23% of 1,1-diphenylmethane diisocyanate polyol pre-polymer. The following samples were prepared:

Shield A consisting of PUR loaded with 20.4% by weight of amorphous boron

Shield C consisting of PUR loaded with 20.9% by weight of boron nitride

Reference shield consisting of pure PUR foil without any filler.

Neutron irradiation of composites

The irradiation was performed in the thermal column of the research reactor TRIGA Mark II at LENA of University of Pavia [48]. The position inside the thermal column employed for the irradiation (next to the BORAL shielding window) presents an integral neutron flux was $1.2 \cdot 10^9$ cm^{-2} s^{-1} with the energy spectrum reported in Table 1 [49].

As reference, a copper wire of certified purity 99.99% was first neutron irradiated in the thermal column. The neutron

Table 1 Neutrons energy spectrum in the thermal column [49]

Neutrons energy by groups (eV)	Measured flux (cm^{-2} s^{-1})
$1 \cdot 10^{-5} \div 4 \cdot 10^{-1}$	$(1.2 \pm 0.1) \cdot 10^9$
$4 \cdot 10^{-1} \div 1 \cdot 10^1$	$(7.5 \pm 0.3) \cdot 10^6$
$1 \cdot 10^1 \div 2 \cdot 10^3$	$(1.2 \pm 0.1) \cdot 10^7$
$2 \cdot 10^3 \div 2 \cdot 10^7$	$(4.4 \pm 0.3) \cdot 10^6$
Integral flux	$(1.2 \pm 0.1) \cdot 10^9$

treatment makes the copper wire radioactive due to the ^{64}Cu radionuclide formation. Without any shielding at the selected neutron fluence the copper wire reaches a reference activity in 3^h30^m irradiation. Afterwards, a series of similar copper wires 99.99% pure were sandwitched between the composite material (see Fig. 1) and irradiated in the thermal column with the same neutron spectra and neutron fluence always given at the nominal thermal power of 250 kW in 3^h30^m. Because of the different thickness and shielding effectiveness of the shielding material, the activity level of the activated copper wires due to the radionuclide ^{64}Cu was found reduced by a certain factor with respect to the activity level achieved by the reference naked copper wire. Through these activity attenuation data measured on the copper wires, following a procedure reported in Ref. [50], two parameters were determined for each composite tested: the linear attenuation coefficient μ (expressed in cm^{-1}) and the mass attenuation coefficient **μ/ρ** expressed in cm^2/g.

Results and discussion

Determination of the linear and mass attenuation coefficient for each composite used as shield

For the radiation fields of indirectly ionizing radiation, such as gamma and neutron radiation, the linear attenuation coefficient μ of a material is defined as the radiation interaction probability of per path unit:

$$I(x) = I_0 e^{-(\mu/\rho)x} \tag{3}$$

whereas I_0 intensity of the radiation field outside the shield, $I(x)$ intensity of the radiation field after a shield of thickness x (cm), μ linear attenuation coefficient (cm^{-1}).

In order to be able to compare the linear attenuation coefficients of different materials, we introduce the mass attenuation coefficient μ/ρ (cm^2/g) with ρ being the density of the PUR composites.

Fig. 1 Example of the experimental set-up. To follow the gradual activation of the copper wire, a wire was put at the beginning of the composite layers, then between the first and second layer, then between the third and fourth layer and so on
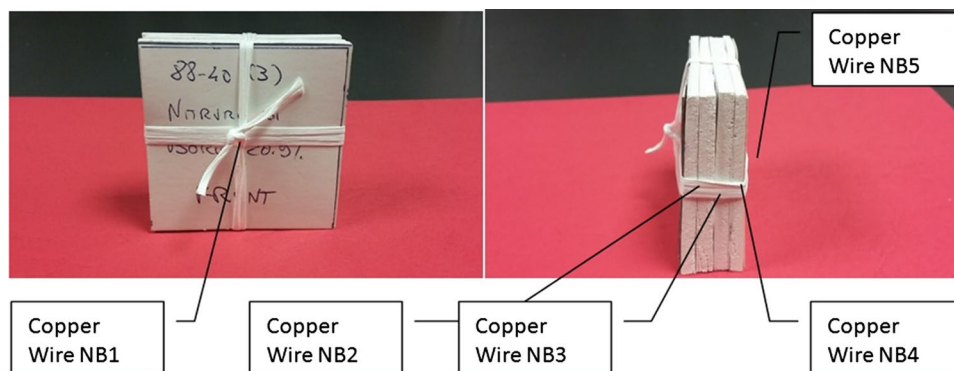
Table 2 Reference shield consisting of pure PUR foils without any filler

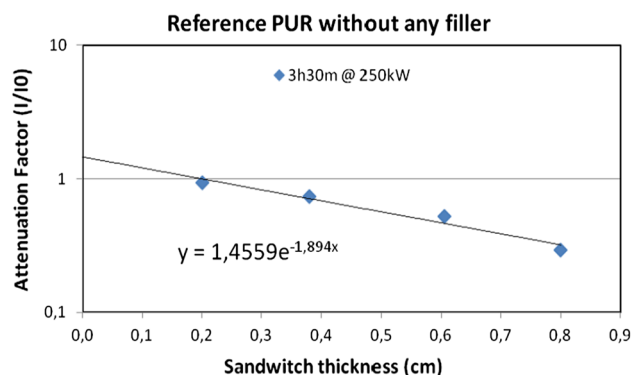| Copper wire id	"Sandwich" thickness (cm)	Specific activity at saturation (Bq/g)	Attenuation factor (I/I₀)
V1 (reference)	0.000	18.2 ± 0.9	–
V2	0.200 ± 0.005	16.9 ± 0.8	0.92 ± 0.09
V3	0.380 ± 0.005	13.4 ± 0.7	0.74 ± 0.07
V4	0.605 ± 0.005	9.5 ± 0.5	0.52 ± 0.05
V4	0.800 ± 0.005	5.3 ± 0.3	0.29 ± 0.03

Fig. 2 The linear attenuation coefficient of unfilled reference PUR was determined from the above graph and found $\mu \sim 1.89$ cm^{-1}. Since the density of the unfilled PUR was measured 1.00 ± 0.04 g cm^{-3} then also the mass attenutation coefficient is $\mu/\rho \sim 1.89$ cm^2 g^{-1}

As first step the neutron attenuation provided by the reference PUR foil without any filler was determined. The results are summarized in Table 2. Essentially, samples of reference PUR of increasing thickness were exposed to the neutron field. The increase in thickness of the radiation shield was achieved simply by overlapping PUR foils and irradiating the copper wire in the shield, measuring the activation by gamma spectrometry and calculating the specific activity at saturation.

From the experimental data regarding the activity of the copper wire (Table 2) and knowing that the total neutron fluence delivered to the samples in 3.5 h was

$$I_0 = 1.51 \times 10^{13} \text{ n/cm}^2$$

the attenuation factor I/I₀ specific for reference unfilled PUR was determined as shown in the last right column of Table 2.

The attenuation factor of the unfilled PUR shield was then plotted against the thickness of the shield as shown in Fig. 2. The data were fitted with an exponential law (see insight the Fig. 2) and the linear attenuation coefficient of $\mu \sim 1.89$ cm^{-1} was determined. Since the density of the unfilled PUR composite was measured 1.00 ± 0.04 g cm^{-3}, then the mass attenuation coefficient of unfilled and reference PUR was found $\mu/\rho \sim 1.89$ cm^2 g^{-1}.

The same procedure was then applied to the PUR composite foils loaded with 20.4% by weight of amorphous boron. Table 3 summarizes all the experimental data regarding the activation of the copper wire till saturation and the resulting attenuation factor.

Following the same procedure employed for the unfilled PUR, the attenuation factor measured on PUR filled with 20.4% of boron were graphed as function of the shield thickness. The data were fitted according to the exponential law yielding a linear attenuation coefficient of $\mu \sim 4.23$ cm^{-1}. Since the density of the PUR composite with 20.4% amorphous boron was measured 0.72 ± 0.03 g cm^{-3}, then the mass attenuation coefficient of PUR filled with 20.4% of boron was found $\mu/\rho \sim 5.87$ cm^2 g^{-1}.

Furthermore, also the PUR composite loaded with 20.9% of h-BN was studied as neutron beam shield.

Table 3 Shield A—PUR loaded with 20.4% by weight of amorph. boron

Copper wire id	"Sandwich" thickness (cm)	Specific activity at saturation (Bq/g)	Attenuation factor (I/I₀)
BA1 (rif.)	0.000	11.8 ± 0.6	–
BA2	0.426 ± 0.005	0.54 ± 0.03	0.045 ± 0.005
BA3	0.806 ± 0.005	0.09 ± 0.01	0.008 ± 0.001
BA4	1.136 ± 0.005	0.03 ± 0.01	0.002 ± 0.001
BA5	1.503 ± 0.005	< 0.01	–

Table 4 Shield C—PUR loaded with 20.9% by weight of boron nitride

Copper wire id	"Sandwich" thickness (cm)	Specific activity at saturation (Bq/g)	Attenuation factor (I/I₀)
NB1 (rif.)	0.000	12.4 ± 0.6	–
NB2	0.351 ± 0.005	1.75 ± 0.08	0.141 ± 0.007
NB3	0.729 ± 0.005	0.35 ± 0.02	0.028 ± 0.001
NB4	1.189 ± 0.005	0.10 ± 0.01	0.008 ± 0.001
NB5	1.497 ± 0.005	< 0.01	–

Table 4 reports all the experimental which were plotted in a graph of the measured attenuation factors as function of the shield thickness. After fitting the data with the exponential law, a linear attenuation coefficient of $\mu \sim 3.44$ cm^{-1} was determined. Since the density of the PUR composite with 20.4% BN was measured 1.02 ± 0.04 g cm^{-3}, then the mass attenuation coefficient of BN filled PUR was found $\mu/\rho \sim 3.37$ cm^2 g^{-1}.

Table 5 summarizes all the linear and mass attenuation coefficients determined. For an easier comparison with the reference value of unfilled PUR, μ and μ/ρ were indexed making 100 the values found on the unfilled PUR. Thus,

Table 5 Summary linear and mass attenuation coefficient of PUR composites

		μ (cm^{-1})	μ/ρ (cm^2/g)	μ (index)	μ/ρ (index)
Ref PUR	Unfilled	1.89	1.89	100	100
Shield A	PUR 20.4% B	4.23	5.87	224	311
Shield C	PUR 20.9% BN	3.44	3.37	182	178

shield A with amorphous boron is 3.1 times more efficient as mass shield against thermal neutrons than reference, while shield C loaded with BN is 1.78 times more efficient than reference. Since the boron amount in BN is only 43.6% of the filler, the real boron load on shield C is only 9.1%. Consequently, the μ/ρ value of shield C is reduced roughly to about half the μ/ρ value of Shield A with 20.4% amorphous boron.

FT-IR spectroscopy of neutron processed composites

The excellent radiation resistance of polyurethanes is known since long time [51]. In fact, it was reported that polyurethanes can resist to a single γ-ray dose of 100 MGy [52] although different polyurethane grades may show different behavior toward high energy radiation [53, 54], which is also affected by the soft and hard segments ratio [54–57]. PUR radiation resistance was also assessed on foams at low temperatures [58].

The PUR matrix employed in our study, is based on polytetrahydrofuran polyol soft segment which is obtained from renewable sources. More precisely, certain biomasses are converted into furfural and the latter into tetrahydrofuran [59] which, through a ring opening polymerization reaction yields the polytetrahydrofuran polyol [60]. Thus, roughly more than 50% of our PUR matrix was derived from such renewable sources.

Based on these premises about the excellent radiation resistance of polyurethanes, certainly much better than PE and moreover of PP [53], it is not a surprise to observe almost no changes in the FT-IR spectra of neutron treated $(1.5 \times 10^{13}$ n cm$^{-2})$ unfilled PUR either front foil of the shield facing the neutron beam or the rear foil behind the shield in comparison to pristine, unfilled PUR, as shown in Fig. 3. The only evident changes are the disappearance of the infrared band at 1261 cm^{-1} observed in the pristine virgin and unfilled PUR in comparison to the neutron-processed
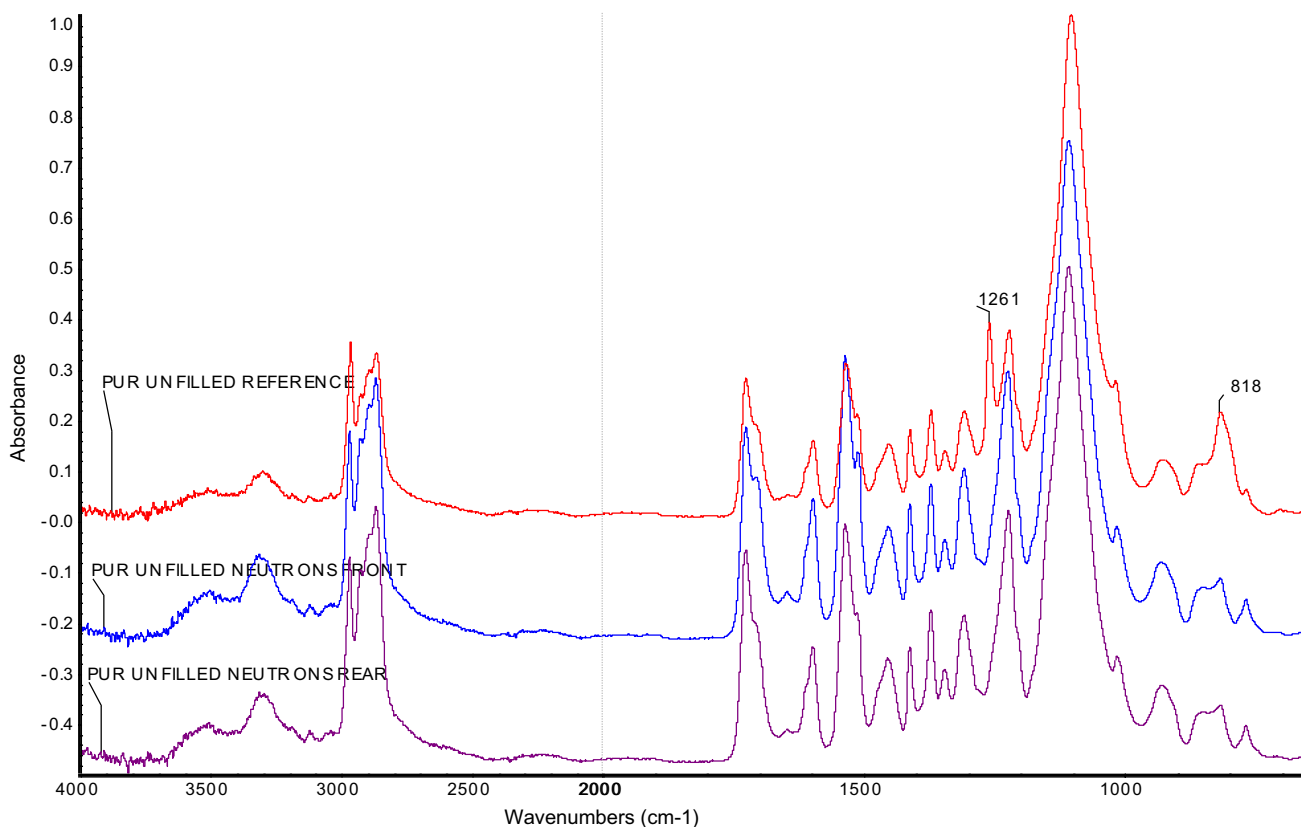

Fig. 3 FT-IR spectra of unfilled polyether-polyurethane; the spectrum in the top (red trace) is due to pristine, virgin unfilled PUR sample; the spectrum in the middle (blue trace) is the unfilled PUR irradiated with neutrons 1.5×10^{13} cm^{-2} (front of the shield); the spectrum at the bottom (violet trace) is the unfilled PUR irradiated with neutrons 1.5×10^{13} cm^{-2} (rear of the shield). (Color figure online)

samples. The band at 1261 cm^{-1} occurs in the CH$_2$ bending and wagging region of PUR [55, 61]. Another small change regards the band at 818 cm^{-1} occurring in the aromatic C–H wagging region [55], which becomes much less prominent in the neutron-processed PUR samples. In the infrared C=O stretching region, the peak at 1705 cm^{-1} is attributed to the hydrogen-bonded C=O while the adjacent peak at 1730 cm^{-1} is assigned to the free and unbounded ketone group [54]. A larger degree of hydrogen bonded ketone group suggests higher degrees of phase separation between hard and soft segments [54]. Figure 3 shows that in the neutron-irradiated PUR a higher intensity of the band at 1730 cm^{-1} with respect to the pristine unirradiated PUR. This may be interpreted in terms of an increase of the free and unbounded C=O group as consequence of neutron irradiation of unfilled PUR. Similarly, also the N–H stretching of PUR is characterized by two infrared bands. The band at lower frequency, namely at about 3300 cm^{-1} is due to hydrogen-bonded N–H groups, whereas the band at 3495 cm^{-1} is instead attributed to the N–H groups not interacting with hydrogen bond [55]. The spectra in Fig. 3 show only that the two infrared bands at 3300 and 3495 cm^{-1} become more intense after the neutron irradiation, the exact meaning of this trend is not clear.

Amorphous boron is not infrared active, although it is Raman active [62]. Thus, there are no specific infrared bands due to the filler in the PUR-amorphous boron composite. The infrared spectrum of boron filled PUR composite is shown in Fig. 4 and is characterized by a prevalence of the 1705 cm^{-1} infrared band intensity over the 1730 cm^{-1} band. The C=O group is more involved in the hydrogen bonding in the boron filled PUR composite than in the unfilled PUR composite. This suggests a stronger polymer-filler compatibility. Similarly, the N–H stretching band at 3300 cm^{-1} involving hydrogen bonding, is more intense in the boron filled PUR composite than in the case of the unfilled PUR. Figure 4 shows that the neutron irradiation enhances the intensity of both the infrared bands at 1705 and at 3300 cm^{-1} suggesting that the neutron irradiation may lead to a further improvement in the polymer-filler interaction. In any case, it is evident that even after the composite processing with 1.5×10^{13} n cm^{-2} there are very little changes in the infrared spectra of the composites, confirming once again the excellent radiation resistance of PUR.

The infrared spectrum of hexagonal boron nitride is dominated by the in-plane B–N stretching band at 1374 cm^{-1}, accompaniend by a weaker out-of-plane B–N–B bending mode at 778 cm^{-1} [36]. Figure 5 shows that the infrared spectrum of boron nitride clearly overlaps to the infrared
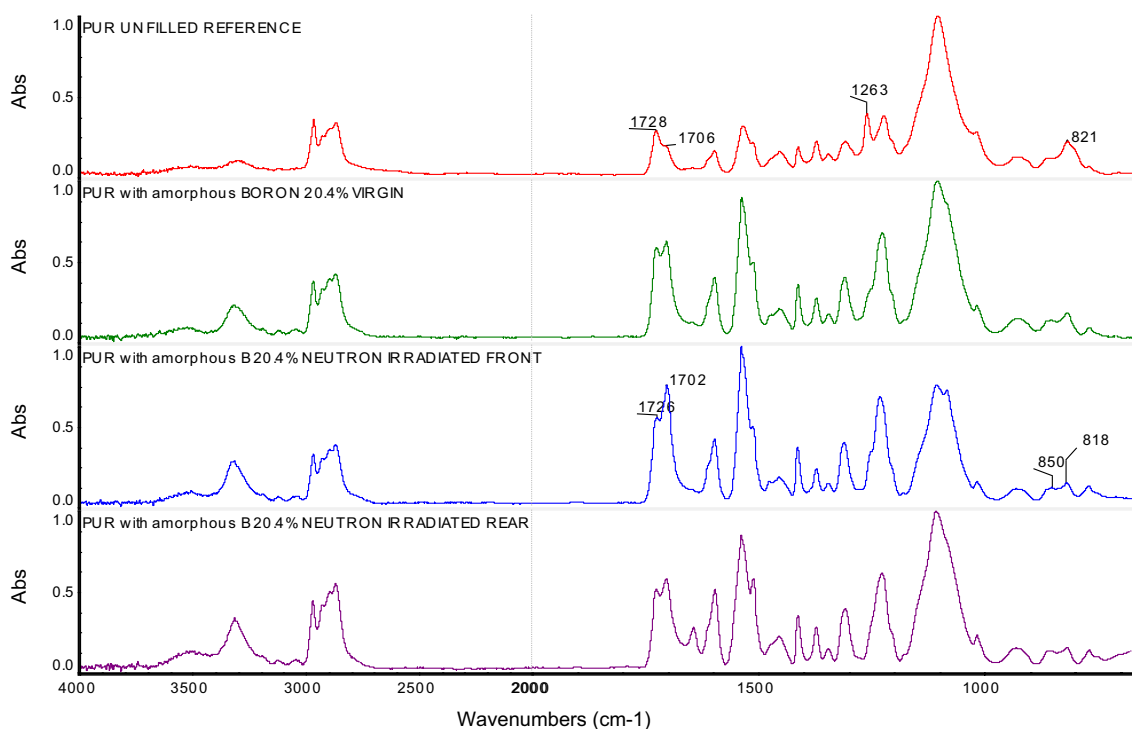

Fig. 4 FT-IR spectra of amorphous boron (20.4%) filled polyether-polyurethane; the spectrum in the top (red trace) is due to pristine, virgin unfilled PUR sample; the second spectrum from top (green trace) is due to amorphous boron filled PUR pristine, not irradiated; the third spectrum from top (blue trace) is due to amorphous boron filled PUR irradiated with neutrons 1.5×10^{13} cm^{-2} (front of the shield); the spectrum at the bottom (violet trace) is due to amorphous boron filled PUR irradiated with neutrons 1.5×10^{13} cm^{-2} (rear of the shield). (Color figure online)
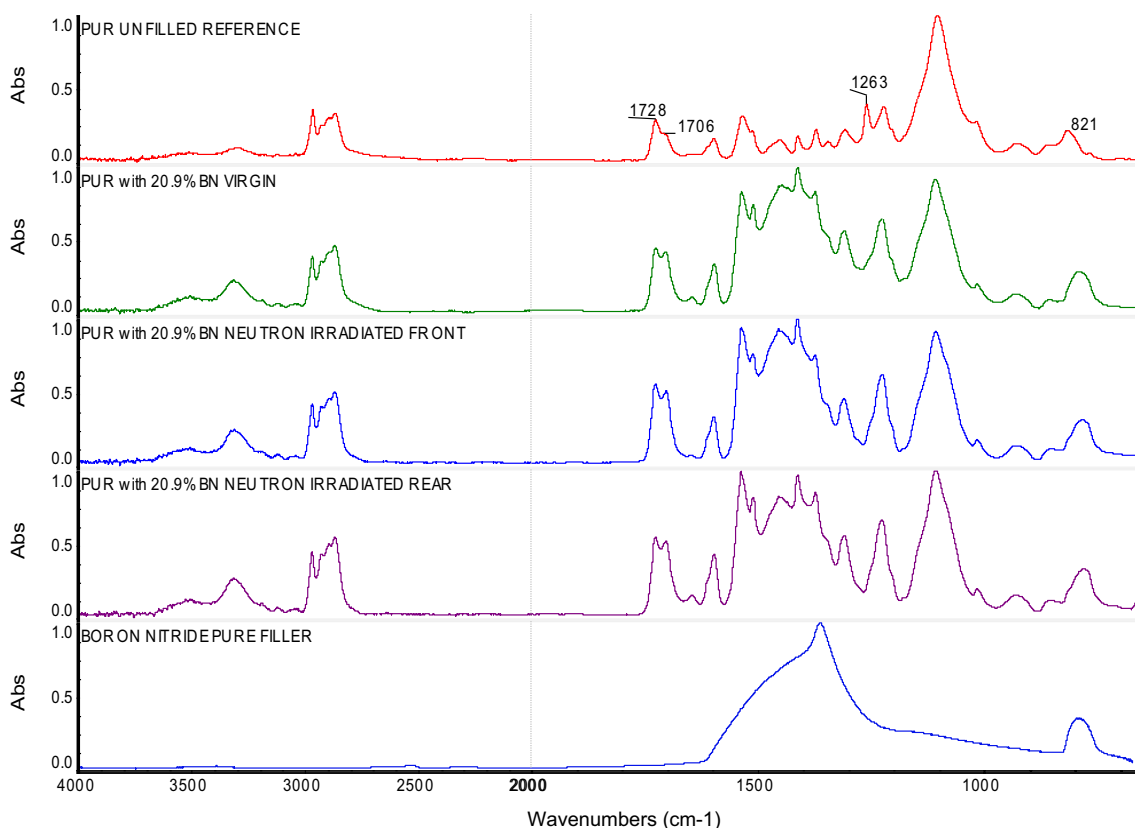
Fig. 5 FT-IR spectra of boron nitride (20.9%) filled polyether-polyurethane; the spectrum in the top (red trace) is due to pristine, virgin unfilled PUR sample; the second spectrum from top (green trace) is due to boron nitride filled PUR pristine, not irradiated; the third spectrum from top (blue trace) is due to boron nitride filled PUR irradiated with neutrons 1.5×10^{13} cm^{-2} (front of the shield); the fourth spectrum from top (violet trace) is due to boron nitride filled PUR irradiated with neutrons 1.5×10^{13} cm^{-2} (rear of the shield); finally, the spectrum at the bottom is due to pure boron nitride filler. (Color figure online)

absorption pattern of PUR matrix. In the BN filled PUR composite the intensity of the two C=O band respectively hydrogen bonded and unbound (i.e. at 1705 and at 1730 cm^{-1} respectively) are of comparable intensity and remain as such even after neutron irradiation. On the other hand, the increase in intensity of the NH stretching band do to hydrogen-bonded NH group after neutron irradiation appears evident also in the case of the BN-filled PUR composite. Also in the case of the latter composite, it is possible to conclude that even after 1.5×10^{13} n cm^{-2} neutron dose there are no significant changes in the infrared spectra of the composite suggesting not only that PUR has a very high radiation resistance, but the presence of BN filles has not at all any deleterious effects.

DSC of neutron processed composites

Differential scanning calorimetry (DSC) is a powerful tool to study the thermal properties of polymers and to investigate also the polymer-filler interaction. The pristine and unfilled PUR used in this study was characterized by a glass transition of -61 °C. Even after neutron irradiation with 1.5×10^{13} n cm^{-2} the Tg did not show any significant shift. Similarly, also the PUR sample filled with 20.4% amorphous boron or with 20.9% of BN shows a Tg$=-61$ °C both in the pristine and in the 1.5×10^{13} cm^{-2} neutron processed sample. Of course a Tg shift may be expected in case of extensive polymer chain scission or in case of extensive crosslinking or both as a consequence of irradiation. Such changes were not observed at all, confirming once again the excellent radiation resistance of the composites studied.

Conclusions

Radiation shielding composites are finding many different applications ranging from nuclear medicine (radiopharmaceuticals preparation and transporation, cyclotron shielding) and cancer radiation therapy to radiology. Shielding is also needed in nuclear reactors, nuclear waste processing, transportation and storage. Emerging technologies which call for challenging radiation shielding are spacecrafts radiation

shielding especially for long term manned missions [4–7] and neutron streaming shielding from fusion Tokamak reactors [8]. Composites offer a wide degree of freedom to taylor-made the shielding material purposely for the selected application and the effective ionizing radiation involved in the given application.

Despite these premises, the typical composites materials employed for shielding are based on PE matrix. Also PMMA and PP are sometimes employed. However other polymer matrices are seldom explored. In this work we have shown that PUR is an excellent polymer matrix for the preparation of thermal neutron shields, but which could be formulated also for the protection of other types of ionizing radiation. PUR offers the advantage of great radiation resistance, it is partly produced from raw materials derived from renewable sources (biomasses) and it can accept high loading of active filler shielding material without adverse effects in the mechanical properties in contrast with the popular PE matrix.

Among the fillers, in this study we have tested both amorphous boron and boron nitride at 21% loading by weight. The resulting composites remain flexible even at these filler loading levels and display excellent shielding properties toward a beam of thermal neutrons in comparison to a reference unloaded PUR composite. As summarized in Table 5 and as expected the PUR composite prepared with amorphous boron shows the best shielding performances followed by PUR composite loaded with BN. The linear and mass attenuation coefficients of the composites were determined and reported in Table 5. The FT-IR and DSC analysis of the unfilled reference PUR and the PUR composites with amorphous B and with BN before and after the neutron processing with a total neutron dose of 1.5×10^{13} cm^{-2}, have confirmed the excellent radiation resistance of the PUR matrix.

References

1. Martin JE (2006) Physics for radiation protection: a handbook. Wiley, New York
2. Stabin MG (2007) Radiation protection and dosimetry: an introduction to health physics. Springer, Berlin
3. Attix FH (2008) Introduction to radiological physics and radiation dosimetry. Wiley, New York
4. Letaw JR, Silberberg R, Tsao CH (1989) Radiation hazards on space missions outside the magnetosphere. Adv Space Res 9:285–291
5. Miroshnichenko L (2003) Radiation hazard in space. Springer, New York
6. Singleterry RC (2013) Radiation engineering analysis of shielding materials to assess their ability to protect astronauts in deep space from energetic particle radiation. Acta Astronaut 91:49–54
7. Campajola L, Di Capua F (2017) Applications of accelerators and radiation sources in the field of space research and industry. Top Curr Chem 374:84
8. Song Y, Wu W, Du S (2014) Tokamak engineering mechanics. Springer, Berlin
9. Wilson JW, Clowdsley MS, Shinn JL, Singleterry RC, Tripathi RK, Cucinotta FA, Heinbockel JH, Badavi FF, Atwell W (2000) Neutrons in space: shield models and design issues (No. 2000-01-2414, 2000). SAE Technical Paper
10. Choppin GR, Rydberg J (1980) Nuclear chemistry. Theory and applications. Pergamon Press, Oxford
11. Filges D, Goldenbaum F (2009) Handbook of spallation research: theory, experiments and applications. Wiley, New York
12. Haffner J (1967) Radiation and shielding in space. Academic Press, New York
13. Woods R, Pikaev A (1994) Applied radiation chemistry: radiation processing. Wiley, New York
14. Guetersloh S, Zeitlin C, Heilbronn L, Miller J, Komiyama T, Fukumura A, Iwata Y, Murakami T, Bhattacharya M (2006) Polyethylene as a radiation shielding standard in simulated cosmic-ray environments. Nucl Instrum Methods Phys Res Sect B Beam Interact Mater Atoms 252:319–332
15. Shin JW, Lee JW, Yu S, Baek BK, Hong JP, Seo Y, Koo CM (2014) Polyethylene/boron-containing composites for radiation shielding. Thermochim Acta 585:5–9
16. Kim J, Lee BC, Uhm YR, Miller WH (2014) Enhancement of thermal neutron attenuation of nano-B$_4$C,-BN dispersed neutron shielding polymer nanocomposites. J Nucl Mater 453:48–53
17. Harrison C, Weaver S, Bertelsen C, Burgett E, Hertel N, Grulke E (2008) Polyethylene/boron nitride composites for space radiation shielding. J Appl Polym Sci 109:2529–2538
18. Jung J, Kim J, Uhm YR, Jeon JK, Lee S, Lee HM, Rhee CK (2010) Preparations and thermal properties of micro-and nano-BN dispersed HDPE composites. Thermochim Acta 499:8–14
19. Mortazavi SMJ, Kardan M, Sina S, Baharvand H, Sharafi N (2016) Design and fabrication of high density borated polyethylene nanocomposites as a neutron shield. Int J Radiat Res 14:379–383
20. İrim ŞG, Wis AA, Keskin MA, Baykara O, Ozkoc G, Avcı A, Dogru M, Karakoç M (2018) Physical, mechanical and neutron shielding properties of h-BN/Gd$_2$O$_3$/HDPE ternary nanocomposites. Radiat Phys Chem 144:434–443
21. Belgin EE, Aycik GA (2015) Preparation and radiation attenuation performances of metal oxide filled polyethylene based composites for ionizing electromagnetic radiation shielding applications. J Radioanal Nucl Chem 306(1):107–117
22. Cummings CS, Lucas EM, Marro JA, Kieu TM, DesJardins JD (2011) The effects of proton radiation on UHMWPE material properties for space flight and medical applications. Adv Space Res 48:1572–1577
23. Zhong WH, Sui G, Jana S, Miller J (2009) Cosmic radiation shielding tests for UHMWPE fiber/nano-epoxy composites. Compos Sci Technol 69:2093–2097
24. Özdemir T, Akbay IK, Uzun H, Reyhancan IA (2016) Neutron shielding of EPDM rubber with boric acid: mechanical, thermal properties and neutron absorption tests. Progr Nucl Energy 89:102–109
25. Huang W, Yang W, Ma Q, Wu J, Fan J, Zhang K (2016) Preparation and characterization of γ-ray radiation shielding PbWO$_4$/EPDM composite. J Radioanal Nucl Chem 309:1097–1103
26. Abdel-Aziz MM, Gwaily SE, Makarious AS, Abdo AES (1995) Ethylene-propylene diene rubber/low density polyethylene/boron carbide composites as neutron shields. Polym Degrad Stab 50:235–240
27. Özdemir T, Güngör A, Reyhancan İA (2017) Flexible neutron shielding composite material of EPDM rubber with boron trioxide: mechanical, thermal investigations and neutron shielding tests. Radiat Phys Chem 131:7–12

28. Mheemeed AK, Hasan HI, Al-Jomaily FM (2012) Gamma-ray absorption using nitrile rubber—lead mixtures as radiation protection shields. J Radioanal Nucl Chem 291:653–659

29. Gwaily SE, Badawy MM, Hassan HH, Madani M (2002) Natural rubber composites as thermal neutron radiation shields: I. B_4C/NR composites. Polym Test 21:129–133

30. Gwaily SE, Hassan HH, Badawy MM, Madani M (2002) Natural rubber composites as thermal neutron radiation shields: II H_3BO_3/NR composites. Polym Test 21:513–517

31. Gwaily SE, Badawy MM, Hassan HH, Madani M (2003) Influence of thermal aging on crosslinking density of boron carbide/natural rubber composites. Polym Test 22:3–7

32. Shaltout NA (2009) Effect of electron beam irradiation and degree of boric acid loading on the properties of styrene-butadiene rubber. React Funct Polym 69:229–233

33. Chai H, Tang X, Ni M, Chen F, Zhang Y, Chen D, Qiu Y (2015) Preparation and properties of flexible flame-retardant neutron shielding material based on methyl vinyl silicone rubber. J Nucl Mater 464:210–215

34. Sukegawa AM, Anayama Y, Okuno K, Sakurai S, Kaminaga A (2011) Flexible heat resistant neutron shielding resin. J Nucl Mater 417:850–853

35. Emmanuel A, Raghavan J (2015) Influence of structure on radiation shielding effectiveness of graphite fiber reinforced polyethylene composite. Adv Space Res 56:1288–1296

36. Cataldo F, Iglesias-Groth S (2017) Neutron damage of hexagonal boron nitride: h-BN. J Radioanal Nucl Chem 313:261–271

37. Cataldo F, Iglesias-Groth S, Hafez Y (2017) Neutron bombardment of boron carbide $B_{12}C_3$: a FT-IR, calorimetric (DSC) and ESR study. Fuller Nanotub Carbon Nanostruct 25:371–378

38. Pascale S, Scatena E, Fabbri F, Cataldo F (2017) Morphological and structural properties of neutron-irradiated $B_{12}C_3$ boron carbide microcrystals. Fuller Nanotub Carbon Nanostruct 25:585–588

39. Cataldo F, Iglesias-Groth S, Prata M (2017) Neutron bombardment of lithium bis (oxalato) borate: LiBOB. J Radioanal Nucl Chem 313:239–247

40. Cataldo F (2000) A Raman study on radiation-damaged graphite by γ-rays. Carbon 38:634–636

41. Cataldo F, Ursini O, Nasillo G, Caponnetti E, Carbone M, Valentini F, Palleschi G, Braun T (2013) Thermal properties, Raman spectroscopy and TEM images of neutron-bombarded graphite. Fuller Nanotub Carbon Nanostruct 21:634–643

42. Cataldo F (2000) On the action of γ radiation on solid C_{60} and C_{70} fullerenes: a comparison with graphite irradiation. Fuller Nanotub Carbon Nanostruct 8:577–593

43. Cataldo F, Baratta GA, Strazzulla G (2002) He^+ ion bombardment of C_{60} fullerene: an FT-IR and Raman study. Fuller Nanotub Carbon Nanostruct 10:197–206

44. Cataldo F, Baratta GA, Ferini G, Strazzulla G (2003) He^+ ion bombardment of C_{70} fullerene: an FT-IR and Raman study. Fuller Nanotub Carbon Nanostruct 11:191–199

45. Iglesias-Groth S, Cataldo F, Hafez Y (2016) Neutron bombardment of C_{60} and C_{70} fullerenes: a spectroscopic and calorimetric study. Fuller Nanotub Carbon Nanostruct 24:547–554

46. Cataldo F, Angelini G, Revay Z, Osawa E, Braun T (2014) Wigner energy of nanodiamond bombarded with neutrons or irradiated with γ radiation. Fuller Nanotub Carbon Nanostruct 22:861–865

47. Cataldo F, Iglesias-Groth S, Hafez Y, Angelini G (2014) Neutron bombardment of single wall carbon nanohorn (SWCNH): DSC determination of the stored Wigner-Szilard energy. J Radioanal Nucl Chem 299:1955–1963

48. Prata M, Alloni D, De Felice P, Palomba M, Pietropaolo A, Pillon M, Quintieri L, Santagata A, Valente P (2014) Italian neutron sources. Eur Phys J Plus 129:255

49. Protti N, Bortolussi S, Prata M, Bruschi P, Altieri S, Nigg D (2012) Neutron spectrometry for the University of Pavia TRIGA™ thermal neutron source facility. Trans Am Nucl Soc 107:1269–1272

50. Alloni D, di Tigliole AB, Bruni J, Cagnazzo M, Cremonesi R, Magrotti G, Oddone M, Panaza F, Prata M, Salvini A (2013) Neutron flux characterization of the SM1 sub-critical multiplying complex of the Pavia University. Progr Nucl Energy 67:98–103

51. Bhowmick AK, Stephens H (eds) (2001) Handbook of elastomers. CRC Press, Boca Raton, p 405

52. Gorna K, Gogolewski S (2003) The effect of gamma radiation on molecular stability and mechanical properties of biodegradable polyurethanes for medical applications. Polym Degrad Stab 79:465–474

53. Tian Q, Takács E, Krakovský I, Horváth Z, Rosta L, Almásy L (2015) Study on the microstructure of polyester polyurethane irradiated in air and water. Polymers 7:1755–1766

54. Walo M, Przybytniak G, Łyczko K, Piątek-Hnat M (2014) The effect of hard/soft segment composition on radiation stability of poly(ester-urethane)s. Radiat Phys Chem 94:18–21

55. Dannoux A, Esnouf S, Begue J, Amekraz B, Moulin C (2005) Degradation kinetics of poly (ether-urethane) Estane® induced by electron irradiation. Nucl Instrum Methods Phys Res Sect B Beam Interact Mater Atoms 236:488–494

56. Wei H, Xiong J, Chen X, Gao X, Xu Y, Fu Y (2007) Study on the radiation degradation of polyether-polyurethane induced by electron beam. J Radioanal Nucl Chem 274:525–530

57. Sui H, Liu X, Zhong F, Li X, Wang B, Ju X (2014) Relationship between free volume and mechanical properties of polyurethane irradiated by gamma rays. J Radioanal Nucl Chem 300:701–706

58. Kim TW, Kim SK, Park S, Park KH, Lee JM (2018) Effect of irradiation on the cryogenic mechanical characteristics of polyurethane foam. J Radioanal Nucl Chem 317:145–159

59. Zeitsch KJ (2000) The chemistry and technology of furfural and its many by-products (vol 13 of sugar series). Elsevier, Amsterdam

60. Cataldo F (1996) Iodine: a ring opening polymerization catalyst for tetrahydrofuran. Eur Polym J 32:1297–1302

61. Murray KA, Kennedy JE, McEvoy B, Vrain O, Ryan D, Cowman R, Higginbotham CL (2013) The influence of electron beam irradiation conducted in air on the thermal, chemical, structural and surface properties of medical grade polyurethane. Eur Polym J 49:1782–1795

62. Werheit H, Filipov V, Kuhlmann U, Schwarz U, Armbrüster M, Leithe-Jasper A, Tanaka T, Higashi I, Lundström T, Gurin VN, Korsukova MM (2010) Raman effect in icosahedral boron-rich solids. Sci Technol Adv Mater 11:023001